Atmos. Chem. Phys., 14, 12803–12814, 2014
www.atmos-chem-phys.net/14/12803/2014/
doi:10.5194/acp-14-12803-2014

Atmospheric Chemistry and Physics
Open Access

On the hiatus in the acceleration of tropical upwelling since the beginning of the 21st century

J. Aschmann[1], J. P. Burrows[1], C. Gebhardt[1], A. Rozanov[1], R. Hommel[1], M. Weber[1], and A. M. Thompson[2]

[1]Institute of Environmental Physics, University of Bremen, Bremen, Germany
[2]NASA/Goddard Space Flight Center, Greenbelt, MD, USA

Correspondence to: J. Aschmann (jan.aschmann@iup.physik.uni-bremen.de)

Received: 19 March – Published in Atmos. Chem. Phys. Discuss.: 17 April 2014
Revised: 27 August 2014 – Accepted: 21 October 2014 – Published: 5 December 2014

Abstract. Chemistry–climate models predict an acceleration of the upwelling branch of the Brewer–Dobson circulation as a consequence of increasing global surface temperatures, resulting from elevated levels of atmospheric greenhouse gases. The observed decrease of ozone in the tropical lower stratosphere during the last decades of the 20th century is consistent with the anticipated acceleration of upwelling. However, more recent satellite observations of ozone reveal that this decrease has unexpectedly stopped in the first decade of the 21st century, challenging the implicit assumption of a continuous acceleration of tropical upwelling. In this study we use three decades of chemistry-transport-model simulations (1980–2013) to investigate this phenomenon and resolve this apparent contradiction. Aside from a high-bias between 1985–1990, our model is able to reproduce the observed tropical lower stratosphere ozone record. A regression analysis identifies a significant decrease in the early period followed by a statistically robust trend-change after 2002, in qualitative agreement with the observations. We demonstrate that this trend-change is correlated with structural changes in the vertical transport, represented in the model by diabatic heating rates taken from the reanalysis product Era-Interim. These changes lead to a hiatus in the acceleration of tropical upwelling between 70–30 hPa and a southward shift of the tropical pipe at 30 and 100 hPa during the past decade, which appear to be the primary causes for the observed trend-change in ozone.

1 Introduction

The issue of whether the large-scale Brewer-Dobson Circulation (BDC) has strengthened in the recent past, as a result of anthropogenic activity, has been raised (Oman et al., 2009; Butchart et al., 2010; Randel and Jensen, 2013). Recent chemistry-climate model (CCM) simulations predict an increase of resolved wave activity and orographic gravity wave drag resulting from increasing sea surface temperatures (SST; Garcia and Randel, 2008; Oman et al., 2009; Waugh et al., 2009; Butchart et al., 2010; Garny et al., 2011). This strengthens the upwelling branch of the BDC, commonly referred to as the tropical upwelling. In comparison, the behaviour of the observations available since about 1980 is ambiguous. The long-term cooling of the tropical lower stratosphere (LS, about 17–21 km; Thompson and Solomon, 2005; Young et al., 2012) and the observed weakening of the stratospheric quasi-biennial oscillation (QBO; Kawatani and Hamilton, 2013) are consistent with the predicted increase of upwelling. On the other hand, the mean residence time of air parcels in the stratosphere (age of air) inferred from sulfur hexafluoride (SF_6) measurements is inconsistent with an overall acceleration of the BDC (Engel et al., 2009; Stiller et al., 2012). Age of air changes indicate no significant changes or even deceleration of the vertical transport in the middle stratosphere. To reconcile the observed discrepancies it has been argued that the individual branches of the BDC are evolving differently, i.e. an increase of tropical upwelling does not necessarily imply an acceleration of the overall circulation (Bönisch et al., 2011; Diallo et al., 2012; Lin and Fu, 2013).

Table 1. Geolocation, temporal coverage and average LS O_3 column of utilised SHADOZ sites.

Name	Location		Coverage	Average [DU]
Ascension Is.	14.4° W	8.0° S	01/1998–08/2010	28.76
Costa Rica	84.0° W	9.9° N	07/2005–12/2012	30.66
Hilo	155.0° W	19.4° N	01/1998–02/2013	36.97
Watukosek-Java	112.6° E	7.5° S	01/1998–06/2013	27.06
Kuala Lumpur	101.7° E	2.7° N	01/1998–12/2011	30.26
Nairobi	36.8° E	1.3° S	01/1998–06/2013	30.66
Natal	35.3° W	5.5° S	01/1998–05/2011	29.74
Paramaribo	55.2° W	5.8° N	09/1999–12/2011	31.53
Samoa	170.6° W	14.2° S	01/1998–12/2012	30.91
San Cristobal	89.6° W	0.9° S	03/1998–10/2008	29.26

Ozone (O_3) is a sensitive proxy for vertical transport in the tropical LS (Randel et al., 2006; Waugh et al., 2009; Randel and Thompson, 2011; Polvani and Solomon, 2012). Its local mixing ratio is considered to result from a stationary state involving production by oxygen (O_2) photo-dissociation and a steady influx of O_3-poor tropospheric air from below (Avallone and Prather, 1996; Waugh et al., 2009; Meul et al., 2014). Meridional mixing from higher latitudes is another factor that contributes to the seasonality in the O_3 mixing ratios (Konopka et al., 2009; Ploeger et al., 2012; Abalos et al., 2013), with the largest impact during boreal summer directly above the tropopause ($\approx$ 380 K/17 km). Several studies have reported a negative trend of O_3 in the tropical LS in the range of $-$(3–6) % per decade from about 1985 onwards, consistent with the CCM predicted increase of tropical upwelling (e.g. Randel and Thompson, 2011; Sioris et al., 2014; Bourassa et al., 2014). In contrast, more recent O_3 observations from various satellite instruments indicate no statistically significant decrease of LS O_3 since the beginning of the 21st century (Kyrölä et al., 2013; Eckert et al., 2014; Gebhardt et al., 2014).

Stimulated by the need to explain the unusual linear trends revealed from the vertical profile of O_3 retrieved from SCIAMACHY we use three decades of O_3 observations and simulations to investigate this phenomenon. Section 2 describes the observations, model and regression analysis used in this study. The results are discussed in Sect. 3.

2 Data and analysis

2.1 Observations

For a quantitative analysis of tropical upwelling, we use combined O_3 observations from satellite instruments and sondes. The earlier decades (1985–2005) are covered by the ERBS/SAGE II instrument (McCormick et al., 1989), providing O_3 profiles based on solar occultation measurements. Due to its viewing geometry, the vertical resolution of the profiles is high (1 km, range 15–50 km), although the horizontal sampling is relatively sparse (global coverage in 1 month). Here we use version 7.0 of the data (Damadeo et al., 2013), screened for cloud and aerosol contaminated profiles as suggested by Wang et al. (2002). Two years of data after June 1991 have been omitted due to contamination by the eruption of Mt. Pinatubo. For the last decade (2002–2012), we use O_3 observations from ENVISAT/SCIAMACHY (Burrows et al., 1995) based on limb geometry (retrieval version 2.9; Sonkaew et al., 2009). The vertical resolution is about 3–4 km over an altitude range of 10–75 km; global coverage is achieved every 6 days. Data from both instruments has been binned into monthly samples on a uniform horizontal and vertical grid (15° lon. $\times$ 5° lat. $\times$ 1 km). To minimise sampling issues and take into account the differences in horizontal and vertical resolution of the instruments, any further analysis is based on partial columns of O_3 between 17–21 km and 20° N–20° S, similar to the approach of Randel and Thompson (2011).

The satellite data is augmented by an ensemble of tropical sonde measurements from the Southern Hemisphere Additional Ozonesondes network (SHADOZ; 1998–2013; Thompson et al., 2003, 2012). We use 10 sites located in the tropics with long and continuous records. The selected stations along with their temporal coverage and mean value are listed in Table 1. Typically there are 2–4 observations per month for each SHADOZ station, which provide O_3 profiles in a considerably higher vertical resolution (50–100 m) compared to the satellite instruments. As there is a high degree of longitudinal symmetry in the stratospheric ozone profiles (Thompson et al., 2003), we average the individual records to obtain a representative mean for the tropics.

2.2 Model

To obtain a consistent time series of LS O_3 of the last decades for direct comparison with observations, we conducted a 33-year simulation with the Bremen three-dimensional chemistry-transport-model (B3DCTM; Sinnhuber et al., 2003; Aschmann et al., 2009; Aschmann and Sinnhuber, 2013). The current version of the model has a

horizontal resolution of 3.75° lon. × 2.5° lat. and covers the vertical domain from the surface up to approximately 55 km using a hybrid $\sigma-\theta$ coordinate system (e.g. Chipperfield, 2006). The vertical resolution in the tropical LS is about 600 m. The model is driven by 6-hourly input of European Centre for Medium-range Weather Forecast (ECMWF) Era-Interim (EI; Dee et al., 2011) reanalysis data. Vertical transport in the purely isentropic domain (above ≈16 km in the tropics) is prescribed by EI all-sky heating rates. The B3DCTM incorporates a comprehensive chemistry scheme originally based on the chemistry part of the SLIMCAT model (Chipperfield, 1999), covering all relevant photochemical reactions for stratospheric O_3 chemistry. Reaction rates and absorption cross-sections are taken from the Jet Propulsion Laboratory recommendations (Sander et al., 2011). Injection of ozone-depleting substances (ODS) is prescribed according to WMO scenario A1 (World Meteorological Organization, 2011). To avoid initialisation artefacts, the model has been run with replicated input data to reach steady state before starting the actual integration from January 1979 to October 2013.

2.3 Regression

The multivariate regression analysis used throughout this study is based on Reinsel et al. (2002) with Y_t as the monthly mean variable to be fitted:

$$\begin{aligned} Y_t &= \mu + S_t + \omega_1 X_{1t} + \omega_2 X_{2t} + \mathrm{QBO}_t + \mathrm{ENSO}_t \\ &\quad + \mathrm{SC}_t + N_t \qquad (1) \\ t &= 1, \ldots, T \end{aligned}$$

where μ is the baseline constant, S_t a seasonal component, $\omega_{1,2}$ are the trend coefficients with $X_{1,2t}$ as trend functions:

$$X_{1t} = t/12 \qquad (2)$$

$$X_{2t} = \begin{cases} 0 & 0 < t \le T_0 \\ (t - T_0)/12 & T_0 < t \le T \end{cases} \qquad (3)$$

Note that in contrast to most previous studies, which examined LS O_3 (e.g. Randel and Thompson, 2011; Sioris et al., 2014), our regression model uses two linear components to take into account a possible change of trend at a given point in time. ω_1 is the linear trend up to a specified inflexion date T_0. After T_0, the new linear trend ω comprises the sum of the earlier trend ω_1 and the trend-change component ω_2. The additional regression terms are QBO_t for QBO, ENSO_t for the El Niño–Southern Oscillation (ENSO) and SC_t for solar cycle. The QBO proxy consists of the QBO.U30 and QBO.U50 (zonal wind 30/50 hPa) from the NOAA Climate Prediction Center[1]; the ENSO proxy is represented by the Multivariate ENSO Index (MEI) from the NOAA Earth System Research Laboratory[2] (Wolter and Timlin, 2011) lagged by 2 months and the solar cycle by the Bremen composite MgII index[3] (Snow et al., 2014). Finally, N_t represents the unexplained noise.

Assuming first order autocorrelation noise (AR(1) model), as commonly used in the regression of O_3 time series (e.g. Reinsel et al., 2002; Jones et al., 2009; Sioris et al., 2014), the corresponding standard deviations for the trend components are given by

$$\sigma_{\omega_1} \approx \frac{\sigma_N}{n^{3/2}} \sqrt{\frac{1+\phi}{1-\phi}} \qquad (4)$$

$$\sigma_{\omega_2} \approx \frac{\sigma_N}{2} \sqrt{\frac{1+\phi}{1-\phi}} \left(\frac{n}{n_0 n_1}\right)^{3/2} \qquad (5)$$

$$\sigma_{\omega} \approx \frac{\sigma_N}{n_1^{3/2}} \sqrt{\frac{1+\phi}{1-\phi}} \sqrt{\frac{n_0 + 4n_1}{4n}} \qquad (6)$$

where σ_N is the standard deviation of the fit residuals, n_0, n_1 are the numbers of years of data before and after the trend-change, respectively, with $n = n_0 + n_1$. ϕ representing the autocorrelation of the residuals with a time lag of 1 month.

The choice of the inflexion year T_0 is a free parameter found in the regression analysis. Figure 1 illustrates the impact of the choice of T_0 on the regression of modelled LS O_3 columns and EI upward mass flux (as discussed below in Sect. 3). A 2σ-significant trend-change (ω_2) is obtained for a range of possible inflexion years (marked by red circles). We therefore use a χ^2 fit based on the regression residuals, similar to the approach described by Jones et al. (2009), to identify the most probable inflexion year. We find a clear minimum in the χ^2 values close to 2002 and consequently select this year as the turning point in the trend analysis.

3 Results and discussion

3.1 Lower stratosphere ozone column

Figure 2 presents tropical LS O_3 column anomalies (20° N–20° S, 17–21 km) from measurements and the simulation. The agreement between model and observations is good, except for a small high-bias relative to the earlier SAGE II data (1985–1990) of approximately 1 DU (≈3 %): correlation coefficients are 0.65 between modelled and observed data sets.

A decline of O_3 is evident in the tropical LS during the first two decades (1980–2002), both in the observed and modelled time series. This is consistent with an increase of tropical upwelling during this period. However, this trend vanishes in the third decade (2002–2013). Figure 3a and b illustrate the results from the regression analysis of the modelled time series showing the fit function and the corresponding residuals, respectively. The linear trend amounts to -8.1 ± 0.9 % per decade (ω_1) in the pre-2002 period and 0.1 ± 3.3 % per

[1] www.cpc.ncep.noaa.gov/data/indices/

[2] www.esrl.noaa.gov/psd/enso/mei/

[3] www.iup.uni-bremen.de/gome/solar/MgII_composite.dat

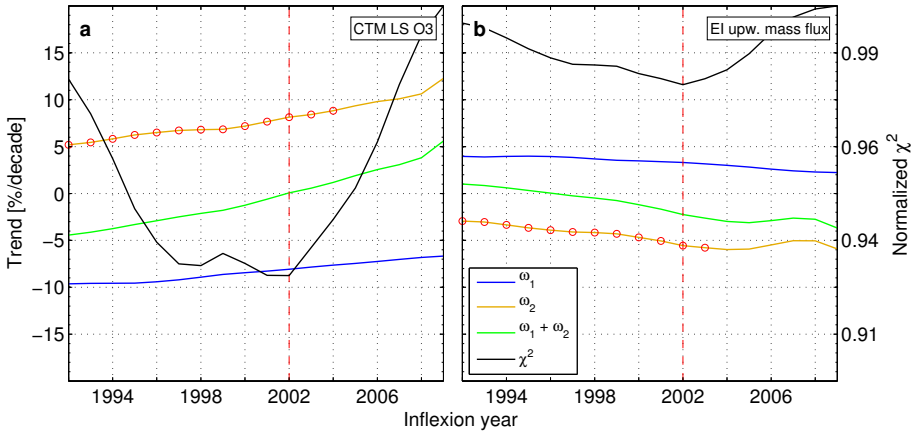

Figure 1. The dependence of the linear fit parameters ω_1, ω_2 and ω ($\omega_1+\omega_2$) on the inflexion year T_0 is shown for the regression of modelled tropical LS O_3 column (**a**) and EI upward mass flux at 70 hPa (**b**). Red circles denote the years where the trend-change (ω_2) exceeds the 95 % confidence threshold. The black lines are the normalised χ^2 values of the fit residuals.

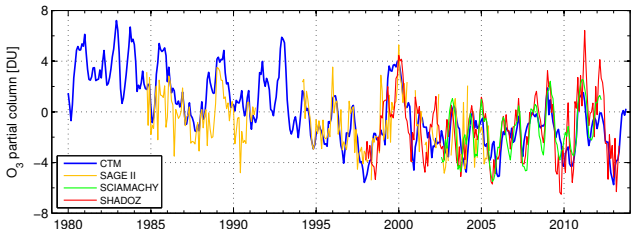

Figure 2. Observed and simulated tropical (20° N–20° S) LS O_3 partial columns (17–21 km). Anomalies are deviations from the modelled 1980–2013 averages.

decade (ω) for the remaining years. The resulting trend-change of 8.2 % per decade (ω_2) is statistically significant within the 95 % confidence interval (i.e. $\omega_2 > 2\sigma_\omega$).

To apply our analysis to the observational data we merge the available data sets (SAGE II–SCIAMACHY; SAGE II–SHADOZ) by joining the two individual time series and average the overlap period. In case of SAGE II–SHADOZ, this method has been applied before by Randel and Thompson (2011), who found excellent agreement between SHADOZ and SAGE II in tropical LS O_3, despite the sparse horizontal sampling provided by the sondes. SAGE II and SCIAMACHY show similarly good agreement in this area, with a correlation of 0.82 and an average bias of 0.5 DU (<2 %) during the overlap period. Considering the good agreement between the observations (Fig. 3), it is reasonable to combine them into a continuous time series. When we apply the regression to the combined SAGE II–SCIAMACHY time series, we calculate a trend of -3.9 ± 0.5 % per decade (ω_1) for the pre-2002 period, consistent with the range of −(3–6) % per decade given by earlier studies (Fig. 3c, d; Randel and Thompson, 2011; Sioris et al., 2014; Bourassa et al., 2014). However, this value is smaller than the pre-2002 trend determined from our CTM simulations. Considering the good agreement between observations and model after the Mt. Pinatubo data gap (1991–1994), the discrepancy must be mainly caused by the model high-bias compared to the early SAGE-II measurements. The origin of this bias is not entirely clear. Assuming that the SAGE II record is consistent before and after the Mt. Pinatubo eruption, the bias possibly results from a spin-up effect of the model stemming from the usage of replicated input data for the initialisation phase (Sect. 2.2). This would explain why the bias is only present in the first third of the time series. Another point could be the systematic overestimation of LS vertical transport based on diabatic heating rates in the EI data set, which is discussed in more detail in Sect. 3.2. After 2002, the agreement between modelled and observed trends improves considerably. For the SAGE II-SCIAMACHY data set, the trend amounts to 0.5 ± 1.5 % per decade (ω), yielding a statistically significant trend- change of 4.4 % per decade (ω_2). We obtain similar values (-3.6 ± 0.5, 0.4 ± 1.4 % per decade for ω_1, ω) if we use the SHADOZ data instead of SCIAMACHY in the combined data set (Fig. 3e, f). Consequently, both observational and model data show that the decrease of LS O_3 effectively stopped around 2002 and there has been no significant change afterwards. This is in qualitative agreement with previous studies, which focus solely on the most recent observational record of O_3. Gebhardt et al. (2014) compared several satellite instruments and report consistently positive trends of tropical O_3 between 17–21 km, ranging from about 2 (OSIRIS), 4 (SCIAMACHY) up to 14 % per decade (MLS), covering the years 2004–2012. Eckert et al. (2014) found a slightly positive trend of 0–1 % per decade in the same region in MIPAS observations (2002–2012). These results cannot be quantitatively compared to our results, as the trends have been calculated for profile ozone and with a significantly different regression approach, which uses only a single linear component and is obviously restricted to 2002/2004–2012.

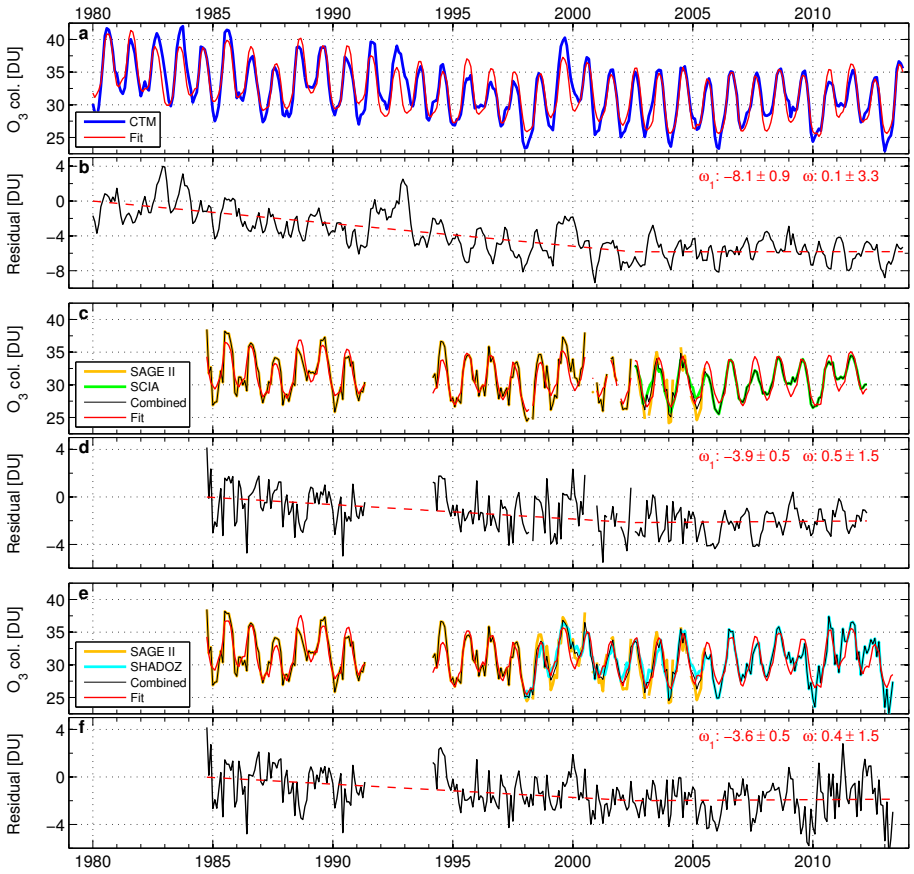

Figure 3. Regression analysis of observed and simulated O_3 partial columns. Model is combined SAGE II/SCIAMACHY and combined SAGE II/SHADOZ LS O_3 with regression function (**a**, **c**, **e**). Corresponding fit residuals excluding the linear terms (**b**, **d**, **f**). The dashed red lines depict the resulting linear trends before and after 2002 with the fit coefficients in red font (unit: % per decade).

If we apply these restrictions to our own regression analysis (i.e. only ω_1, range 2002–2012), the resulting trends are consistent with the earlier studies, i.e. 3–5 % per decade for model and SCIAMACHY profile ozone between 17–21 km in the tropics (not shown here). The important point is, that despite the considerable spread in the determined trends all instruments described above show no further decrease of tropical LS O_3 during the last decade. This agreement justifies our confidence that this phenomenon is not an instrumental or retrieval artefact.

Local chemical effects can be largely ruled out as explanation for the detected trend-change of LS O_3. As stated above, O_3 abundance in the tropical LS is mainly determined by vertical transport and chemical net production (by O_2 photolysis; Avallone and Prather, 1996; Waugh et al., 2009; Meul et al., 2014). O_3-destroying catalytic species are scarce in the tropical LS, therefore the phase-out of ODS, and the associated recovery (e.g. World Meteorological Organization, 2011), has no direct impact on O_3 concentrations in this region. To verify this assumption, we have conducted a sensitivity simulation with identical setup but with ODS emissions fixed to the values of 1980 (not shown here). In contrast to mid and high latitudes, the O_3 mixing ratios in the tropical LS show little difference to the standard simulation (<2 % compared to 15–20 % at higher latitudes) and we calculate very similar trends (-7.8 ± 0.9, -0.6 ± 3.4 % per decade for ω_1, ω). The relatively small impact on the post-2002 trend ω, compared to the overall trend-change, is likely related to O_3 in-mixing from mid-latitudes. Not explicitly accounted for is a possible indirect relationship between ODS-related polar O_3 depletion and tropical LS O_3 by dynamical coupling, as pointed out by several studies (Waugh et al., 2009; Oman et al., 2009). Furthermore, the model does not consider in-mixing of extra-tropical pollutants aside from ODS. Meul et al. (2014) predict an increase of photolytic O_3 production as a result from long-term changes in the overhead O_3 column. Furthermore, an increase of odd nitrogen (NO_x) might lead to additional O_3 production. However, they found no indication that either process is sufficient to explain a short-term trend-change. Overall the most probable explanation of the observed behaviour is that changes in dynamics must be involved.

3.2 Tropical upwelling

On the dynamical side, the obvious impact factors are tropical upwelling and in-mixing from higher latitudes. An accurate attribution of the relative impact of each process is difficult, as they are not completely independent from each other. From an Eulerian point of view, changes in the vertical flux must be balanced by horizontal exchange due to mass conservation. From a Lagrangian perspective, the vertical velocity of an air parcel determines the effectiveness of a local in-mixing region, for example by the Asian monsoon anticyclone as described by Ploeger et al. (2012); Abalos et al. (2013). In the following, we concentrate on tropical upwelling as it is easier to quantify than in-mixing. A typical representative quantity for the tropical upwelling is the upward mass flux at 70 hPa (≈18.5 km in the tropics; Butchart et al., 2010; Seviour et al., 2012). A recent study assessing the upward mass flux in EI found a negative trend of −5 % per decade for the years 1989–2009, based on EI kinematic vertical winds (Seviour et al., 2012). This is in contradiction with the results of current CCMs, which predict an increase of upwelling of about 2.0 % per decade (ensemble mean; Butchart et al., 2010). The quality of stratospheric vertical transport in EI improves considerably, when diabatic heating rates are used instead of the kinematic wind. The diabatic representation of vertical transport generally yields more realistic estimates of stratospheric age of air in comparison to the kinematic approach (Diallo et al., 2012) and is also less dispersive (Ploeger et al., 2011). On the downside, there are indications that EI heating rates overestimate the ascent in the tropics. Diallo et al. (2012) report an underestimation of age of air compared to observations in the tropical Northern Hemisphere, reaching up to 50 % when using EI heating rates. Similarly, Fueglistaler et al. (2009) and Ploeger et al. (2012) state that EI heating rates are too fast by 40–50 % in the tropical upper troposphere/lower stratosphere (UTLS). According to Fueglistaler et al. (2009), a significant part of this overestimation can be attributed to the fixed O_3 climatology for calculating the heating rates in the reanalysis. As the utilised climatology by Fortuin and Langematz (1995) is based on data from 1966–1990 and the real O_3 mixing ratio decreases until 2002 (Sect. 3.1), this will lead to increasingly biased responses of the EI radiative transfer scheme during this period. This would partly explain the overestimation of the pre-2002 trend of LS O_3 in the model (Sect. 3.1) and is consistent with the similar overestimation of the upwelling trend in EI discussed below.

Figure 4 shows the tropical LS EI all-sky heating rates (20° N–20° S, 17–21 km; panel a), which are used to drive the vertical transport in our isentropic model, and the corresponding EI upward mass flux at 70 hPa (panel c). The upward mass flux is the integral of the residual vertical velocity w^* between turnaround latitudes (ϕ^{SH}, ϕ^{NH}) as described in Seviour et al. (2012)

$$\text{upward mass flux} = 2\pi \int_{\phi^{SH}}^{\phi^{NH}} w^* \rho_0 a^2 \cos\phi \; d\phi \qquad (7)$$

with basic state density ρ_0 and Earth's radius a. In turn, w^* is calculated from the EI heating rates using the iterative algorithm described by Solomon et al. (1986). Applying the regression analysis to the upward mass flux yields a positive trend of 3.3 ± 0.7 % per decade for the pre-2002 period (ω_1; Fig. 4d). This value is consistent with the CCM results (2.0 % per decade) although somewhat high-biased, likely reflecting the impact of the fixed O_3 climatology for calculating the EI heating rates as discussed above. After 2002, however, there is a statistically significant trend-change leading to a negative trend of -2.3 ± 2.5 % per decade (ω), mirroring the trend-change in the LS O_3 time series.

3.3 Structural BDC changes

Further insight into structural changes of the BDC can be gained by decomposing the circulation into different branches. Here, we adopt the method of Lin and Fu (2013) and define the tropically controlled transition branch, ranging from 100 to 70 hPa and the stratospheric shallow and deep branch (70–30 hPa and <30 hPa, respectively). The strength of the individual branches is estimated by the differences of upward mass fluxes across the corresponding boundaries (determined between turnaround latitudes); in the case of the deep branch, it is simply the flux across the 30 hPa boundary. Figure 5 presents the results of the regression analysis of the mass fluxes in the individual branches, calculated from EI all-sky heating rates as above. In the stratospheric deep branch, there is no significant non-zero trend during the last decades, which is consistent with earlier studies (e.g. Engel et al., 2009; Bönisch et al., 2011; Lin and Fu, 2013). Consequently, the evolution of the shallow branch is dominated by the changes in the 70 hPa flux as discussed above (Fig. 4d), displaying the characteristic trend-change around 2002 (5.8 ± 0.9, -5.6 ± 3.3 % per decade for ω_1, ω). Interestingly, the transition branch shows the inverted behaviour, a decrease prior to 2002 and an increase afterwards (-9.0 ± 1.1, 11.1 ± 4.0 % per decade for ω_1, ω). Apparently there is a shift in mass flux balance from the transition branch towards the shallow branch in earlier decades, which begins to reverse at the beginning of the 21st century. This result does not agree with the findings of Lin and Fu (2013), who calculate positive trends both in the transition and shallow branches based on current CCM simulations. However, Bönisch et al. (2011) detect a significant increase of the residual circulation around 2000, based on N_2O and O_3 observations. They state that this increase is mainly confined to the lower stratosphere between 100–63 hPa, which is consistent with our definition of the transition branch.

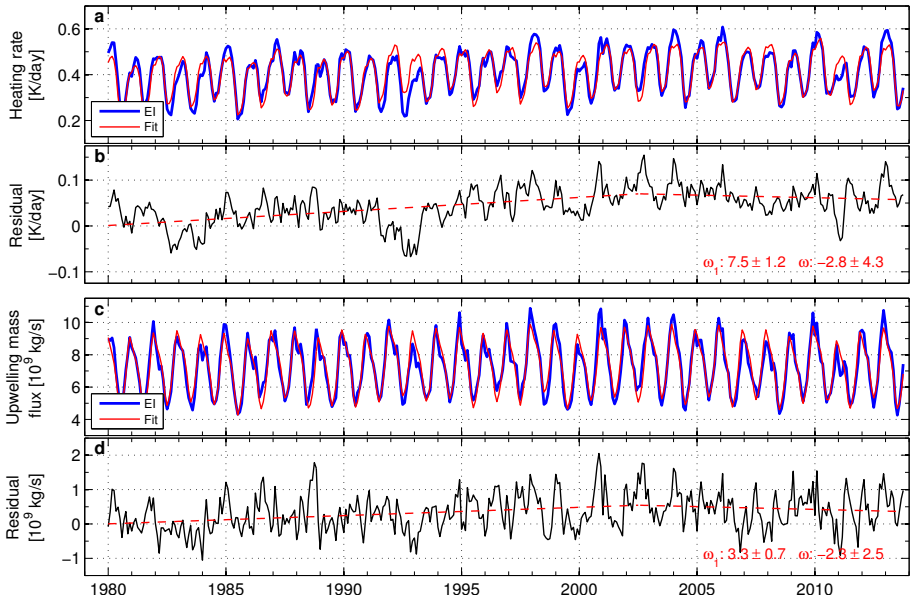

Figure 4. Regression analysis of EI LS all-sky heating rate (17–21 km; **a, b**) and upwelling mass flux (70 hPa; **c, d**). Setup identical to Fig. 3 otherwise.

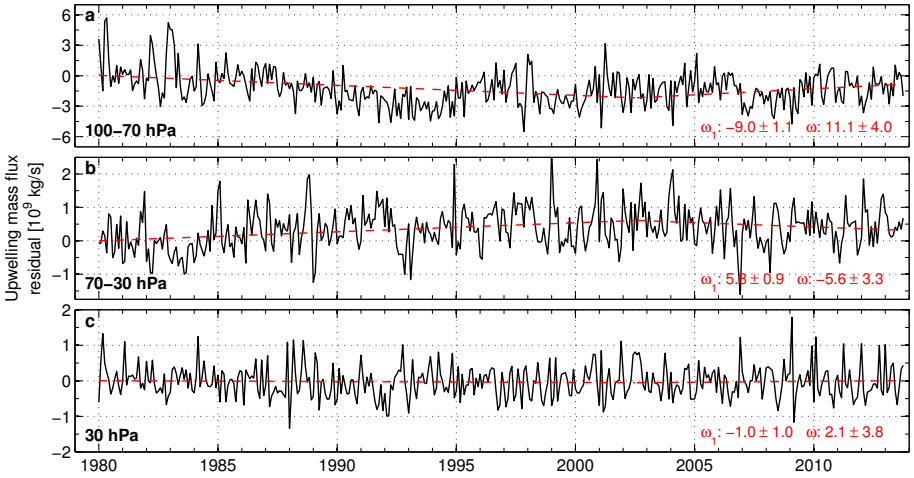

Figure 5. Fit residuals (excluding linear terms) of EI upwelling mass fluxes in different BDC branches (**a** 100–70 hPa; **b** 70–30 hPa; **c** 30 hPa). The dashed red lines depict the resulting linear trends before and after 2002 with the fit coefficients in red font (unit: % per decade).

Another important aspect is the evolution of the tropical mixing barriers, i.e. the extent of the "tropical pipe" (Plumb, 1996). Stiller et al. (2012) and Eckert et al. (2014) state that the observed trend patterns of SF_6 and O_3 could be possibly explained by a weakening or a shift of transport barriers. In turn, the extent of the tropical pipe is affected by the same dynamical processes which cause the increase in tropical upwelling (Li et al., 2010). Therefore it is likely that both phenomena are related. Figure 6 shows the development of the turnaround latitudes determined from upward mass fluxes at 100, 70 and 30 hPa, separated for the Northern and Southern Hemisphere (NH, SH). The resulting linear trends are listed in Table 2. The tropical pipe is expanding at all three levels in the pre-2002 period. In the 100 and 30 hPa level the expansion is about 2.7° per decade whereas the trend in the NH is roughly twice as large as in the SH. At 70 hPa, the expansion is only 0.6° per decade, mainly restricted to the SH as there is no significant trend in the NH. After 2002, the tropical pipe shrinks at all levels. Again, the effect is most pronounced at 100 and 30 hPa with −6.2° per decade and −2.8° per decade, respectively and there is the same asymmetry that the change is much stronger in the NH. At 70 hPa, the effect is smaller (−0.8° per decade) and restricted to the SH. The development at the lowermost level (100 hPa) is consistent with the observed widening of the tropical belt in the troposphere (Seidel et al., 2008). Relying on independent observational

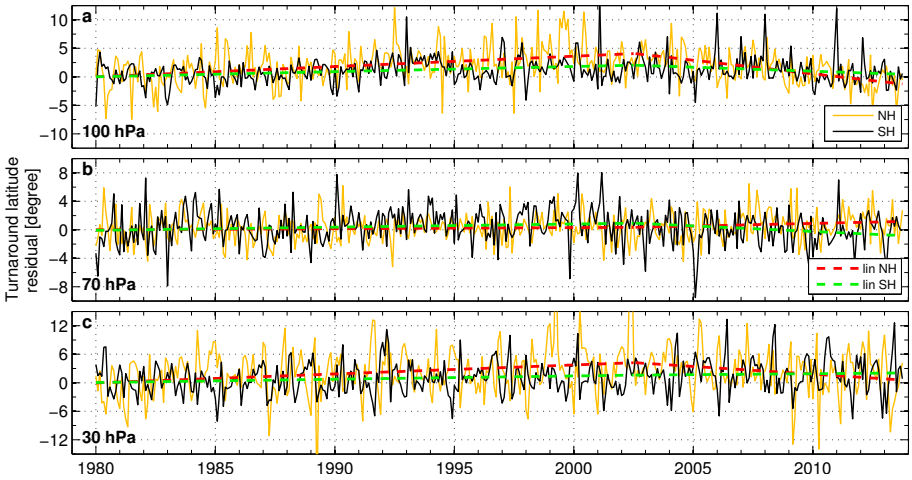

Figure 6. Fit residuals (excluding linear terms) of turnaround latitudes determined from EI upwelling mass fluxes at different pressure levels (**a** 100 hPa; **b** 70 hPa; **c** 30 hPa). The black and orange lines denote the fit residuals whereas the red and green dashed lines depict the resulting linear trends in the Northern and Southern Hemisphere (NH/SH), respectively.

Table 2. Average turn-around latitude per level and hemisphere and corresponding linear trend coefficients obtained from the regression analysis (Fig. 6). The unit of the trends is degree per decade.

p [hPa]	∅ [°]	ω_1	ω_2	ω
NH 100	21.9	1.81 ± 0.15	-6.58 ± 0.73	-4.77 ± 0.56
SH 100	18.6	0.90 ± 0.13	-2.31 ± 0.62	-1.41 ± 0.48
NH 70	31.4	0.16 ± 0.10	0.58 ± 0.47	0.74 ± 0.37
SH 70	29.8	0.44 ± 0.13	-2.01 ± 0.63	-1.56 ± 0.49
NH 30	37.5	1.89 ± 0.34	-5.14 ± 1.60	-3.25 ± 1.24
SH 30	32.1	0.69 ± 0.23	-0.29 ± 1.11	0.41 ± 0.86

parameters, they state that the tropical belt expanded by 2–5° per decade between 1980–2005. The expansion accompanying the mass flux decrease in the pre-2002 period and the inverted picture afterwards is also in agreement with the findings of Li et al. (2010), who predict an anti-correlation between upwelling strength and expansion of tropical mixing barriers. However, we cannot reproduce this anti-correlation at 70 and 30 hPa. At 70 hPa, there is hardly any statistically significant change in the extent of the tropical pipe although the mass flux is changing whereas Li et al. (2010) predict a narrowing at the same pressure level of −0.5° per decade. Just the opposite situation occurs at 30 hPa. Here, the extent of the tropical pipe is changing despite the absence of significant vertical mass flux changes. An interesting detail is the south-shift of the tropical pipe after 2002. Both at 100 hPa and 30 hPa there is a net south-shift of tropical upwelling of 3.4–3.7° per decade, which is in good agreement with the estimated south-shift of 5° on the basis of MIPAS O_3 observations (2002–2012; Eckert et al., 2014).

4 Discussion and conclusions

In this study, we compile observations and model simulations of tropical LS O_3 from 1980–2013. We find negative trends of O_3 both in observation and model before 2002, consistent with earlier studies (e.g. Randel and Thompson, 2011). These trends in O_3 are accompanied by an increase of tropical upwelling found in the EI data set based upon diabatic heating calculation, confined to the shallow branch of the BDC (70–30 hPa). This is also in agreement with previous modelling studies, which predict an increase of upwelling (e.g. Butchart et al., 2010). However, we also find an unexpected hiatus of the negative trend in LS O_3 after 2002, mirrored by a similar feature in the behaviour of the vertical transport in the EI data set. Our analysis shows that the acceleration of the shallow branch has ceased; at the same time the strength of the transition branch (100–70 hPa) increases after about 2002, in agreement with the findings of Bönisch et al. (2011). The deep branch (<30 hPa) does not show any significant changes. We further see an expansion of the tropical pipe before 2002, followed by a narrowing afterwards. This effect is most pronounced at 100 and 30 hPa, where the upwelling is shifted also northwards before and southwards after 2002.

Taking into account the sensitivity of LS O_3 to vertical transport, there are strong indications that the observed trend-change in O_3 is primarily a consequence of the simultaneous trend-change in tropical upwelling. As the analysed partial columns are dominated by the upper altitudes due to the steep vertical gradient in tropical O_3, they are particularly sensitive to changes in the shallow branch of the BDC between 70–30 hPa. This hypothesis is corroborated by significant anti-correlation between LS O_3 anomalies with either heating rates (−0.83), or 70 hPa upward mass flux anoma-

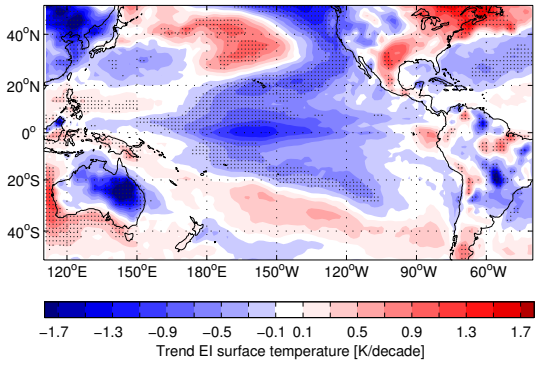

Figure 7. Linear trends of EI surface temperature from 2002–2013. Stippling indicates where the trend exceeds the 95% confidence threshold. Setup adapted from Kosaka and Xie (2013).

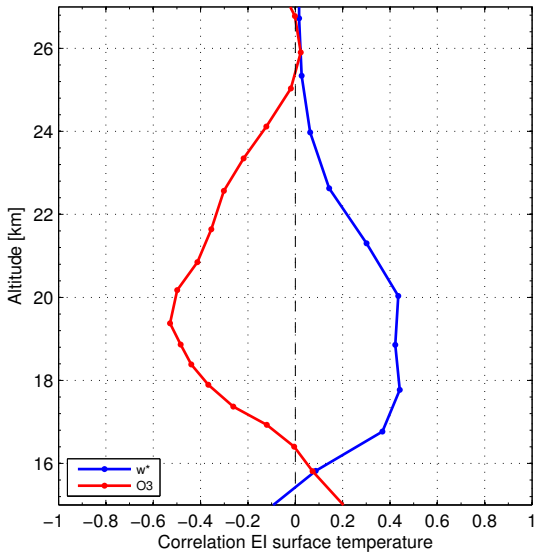

Figure 8. Correlation of EI surface temperature anomalies with anomalies of w^* calculated from EI all-sky heating rates and modelled O_3 mixing ratios in the tropics (20° N–20° S). The corresponding time series range from 01-1980 to 10-2013.

lies (−0.55). However, we cannot rule out a possible impact of in-mixing, which is not covered by our analysis. Further, the detected southward shift of upwelling after 2002 in the EI data set is consistent with the hypothesis of Eckert et al. (2014), who demonstrated that the recently observed O_3 trends could be partly explained by a south-shift of the tropical mixing barriers. This is not necessarily a contradiction to our conclusion, as both upwelling and location of mixing barriers are impacted by the same dynamical processes (Li et al., 2010).

The cause of these changes is currently unknown. One plausible explanation could be the unexpected La-Niña-like cooling of the equatorial Eastern Pacific since the beginning of the 21st century (Meehl et al., 2011). The cause of this cooling is not yet fully understood and currently debated (Chen and Tung, 2014). However, it has a significant impact on global surface temperatures (Kosaka and Xie, 2013) and ultimately, by dynamical coupling, on tropical upwelling (Oman et al., 2009; Butchart et al., 2010; Garny et al., 2011). Recent studies describe the associated circulation changes (England et al., 2014) and their impact on tropospheric O_3 (Lin et al., 2014). In contrast to current unconstrained CCM, which generally do not predict this exceptional cooling of the equatorial Eastern Pacific surface (Kosaka and Xie, 2013; England et al., 2014), this feature can be clearly observed in the data-assimilated EI data set (Fig. 7). This hypothesis is further corroborated by significant (anti-) correlation between tropical surface temperatures and LS upwelling/O_3 mixing ratios, which is most prominent in the LS (Fig. 8; Hardiman et al., 2007). This particular relationship between ocean and atmosphere must be investigated in more detail, as it is likely that the accuracy of our predictions of future BDC development and its consequences for stratospheric O_3 critically depends on our understanding of this interaction.

Acknowledgements. This study has been funded in part by the University and State of Bremen, the DFG Research Unit 1095 Stratospheric Change and its Role for Climate Prediction, SHARP, and the German Federal Ministry of Education and Research, research project Role Of the Middle atmosphere In Climate (ROMIC). SHADOZ, the Southern Hemisphere Additional Ozonesondes network, is funded by NASA's Upper Atmosphere Research Program. We thank G. Stiller and the three anonymous referees for their help in improving the manuscript.

Edited by: M. Dameris

References

Abalos, M., Ploeger, F., Konopka, P., Randel, W. J., and Serrano, E.: Ozone seasonality above the tropical tropopause: reconciling the Eulerian and Lagrangian perspectives of transport processes, Atmos. Chem. Phys., 13, 10787–10794, doi:10.5194/acp-13-10787-2013, 2013.

Aschmann, J. and Sinnhuber, B.-M.: Contribution of very short-lived substances to stratospheric bromine loading: uncertainties and constraints, Atmos. Chem. Phys., 13, 1203–1219, doi:10.5194/acp-13-1203-2013, 2013.

Aschmann, J., Sinnhuber, B.-M., Atlas, E. L., and Schauffler, S. M.: Modeling the transport of very short-lived substances into the tropical upper troposphere and lower stratosphere, Atmos. Chem. Phys., 9, 9237–9247, doi:10.5194/acp-9-9237-2009, 2009.

Avallone, L. M. and Prather, M. J.: Photochemical evolution of ozone in the lower tropical stratosphere, J. Geophys. Res.-Atmos., 101, 1457–1461, doi:10.1029/95JD03010, 1996.

Bönisch, H., Engel, A., Birner, Th., Hoor, P., Tarasick, D. W., and Ray, E. A.: On the structural changes in the Brewer-Dobson circulation after 2000, Atmos. Chem. Phys., 11, 3937–3948, doi:10.5194/acp-11-3937-2011, 2011.

Bourassa, A. E., Degenstein, D. A., Randel, W. J., Zawodny, J. M., Kyrölä, E., McLinden, C. A., Sioris, C. E., and Roth, C.

Z.: Trends in stratospheric ozone derived from merged SAGE II and Odin-OSIRIS satellite observations, Atmos. Chem. Phys., 14, 6983–6994, doi:10.5194/acp-14-6983-2014, 2014.

Burrows, J., Hölzle, E., Goede, A., Visser, H., and Fricke, W.: SCIAMACHY – scanning imaging absorption spectrometer for atmospheric chartography, Acta Astronaut., 35, 445–451, doi:10.1016/0094-5765(94)00278-T, 1995.

Butchart, N., Cionni, I., Eyring, V., Shepherd, T. G., Waugh, D. W., Akiyoshi, H., Austin, J., Bruehl, C., Chipperfield, M. P., Cordero, E., Dameris, M., Deckert, R., Dhomse, S., Frith, S. M., Garcia, R. R., Gettelman, A., Giorgetta, M. A., Kinnison, D. E., Li, F., Mancini, E., McLandress, C., Pawson, S., Pitari, G., Plummer, D. A., Rozanov, E., Sassi, F., Scinocca, J. F., Shibata, K., Steil, B., and Tian, W.: Chemistry-climate model simulations of twenty-first century stratospheric climate and circulation changes, J. Climate, 23, 5349–5374, doi:10.1175/2010JCLI3404.1, 2010.

Chen, X. and Tung, K.-K.: Varying planetary heat sink led to global-warming slowdown and acceleration, Science, 345, 897–903, doi:10.1126/science.1254937, 2014.

Chipperfield, M. P.: Multiannual simulations with a three-dimensional chemical transport model, J. Geophys. Res.-Atmos., 104, 1781–1805, 1999.

Chipperfield, M. P.: New version of the TOMCAT/SLIMCAT off-line chemical transport model: intercomparison of stratospheric tracer experiments, Q. J. Roy. Meteor. Soc., 132, 1179–1203, doi:10.1256/qj.05.51, 2006.

Damadeo, R. P., Zawodny, J. M., Thomason, L. W., and Iyer, N.: SAGE version 7.0 algorithm: application to SAGE II, Atmos. Meas. Tech., 6, 3539–3561, doi:10.5194/amt-6-3539-2013, 2013.

Dee, D. P., Uppala, S. M., Simmons, A. J., Berrisford, P., Poli, P., Kobayashi, S., Andrae, U., Balmaseda, M. A., Balsamo, G., Bauer, P., Bechtold, P., Beljaars, A. C. M., van de Berg, L., Bidlot, J., Bormann, N., Delsol, C., Dragani, R., Fuentes, M., Geer, A. J., Haimberger, L., Healy, S. B., Hersbach, H., Hólm, E. V., Isaksen, L., Kållberg, P., Köhler, M., Matricardi, M., McNally, A. P., Monge-Sanz, B. M., Morcrette, J.-J., Park, B.-K., Peubey, C., de Rosnay, P., Tavolato, C., Thépaut, J.-N., and Vitart, F.: The ERA-Interim reanalysis: configuration and performance of the data assimilation system, Q. J. Roy. Meteor. Soc., 137, 553–597, doi:10.1002/qj.828, 2011.

Diallo, M., Legras, B., and Chédin, A.: Age of stratospheric air in the ERA-Interim, Atmos. Chem. Phys., 12, 12133–12154, doi:10.5194/acp-12-12133-2012, 2012.

Eckert, E., von Clarmann, T., Kiefer, M., Stiller, G. P., Lossow, S., Glatthor, N., Degenstein, D. A., Froidevaux, L., Godin-Beekmann, S., Leblanc, T., McDermid, S., Pastel, M., Steinbrecht, W., Swart, D. P. J., Walker, K. A., and Bernath, P. F.: Drift-corrected trends and periodic variations in MIPAS IMK/IAA ozone measurements, Atmos. Chem. Phys., 14, 2571–2589, doi:10.5194/acp-14-2571-2014, 2014.

Engel, A., Moebius, T., Bönisch, H., Schmidt, U., Heinz, R., Levin, I., Atlas, E., Aoki, S., Nakazawa, T., Sugawara, S., Moore, F., Hurst, D., Elkins, J., Schauffler, S., Andrews, A., and Boering, K.: Age of stratospheric air unchanged within uncertainties over the past 30 years, Nat. Geosci., 2, 28–31, doi:10.1038/NGEO388, 2009.

England, M. H., McGregor, S., Spence, P., Meehl, G. A., Timmermann, A., Cai, W., Gupta, A. S., McPhaden, M. J., Purich, A., and Santoso, A.: Recent intensification of wind-driven circulation in the Pacific and the ongoing warming hiatus, Nat. Clim. Change, 4, 222–227, doi:10.1038/nclimate2106, 2014.

Fortuin, J. and Langematz, U.: An update on the global ozone climatology and on concurrent ozone and temperature trends, in: Atmospheric sensing and modeling, edited by Santer, R. P., vol. 2311 of Proceedings of the society of Photo-optical Instrumentation Engineers (SPIE), 207–216, Conference on Atmospheric Sensing and Modeling, Rome, Italy, 29–30 September 1994, 1995.

Fueglistaler, S., Legras, B., Beljaars, A., Morcrette, J.-J., Simmons, A., Tompkins, A. M., and Uppala, S.: The diabatic heat budget of the upper troposphere and lower/mid stratosphere in ECMWF reanalyses, Q. J. Roy. Meteor. Soc., 135, 21–37, doi:10.1002/qj.361, 2009.

Garcia, R. R. and Randel, W. J.: Acceleration of the Brewer–Dobson circulation due to increases in greenhouse gases, J. Atmos. Sci., 65, 2731–2739, doi:10.1175/2008JAS2712.1, 2008.

Garny, H., Dameris, M., Randel, W., Bodeker, G. E., and Deckert, R.: Dynamically forced increase of tropical upwelling in the lower stratosphere, J. Atmos. Sci., 68, 1214–1233, doi:10.1175/2011JAS3701.1, 2011.

Gebhardt, C., Rozanov, A., Hommel, R., Weber, M., Bovensmann, H., Burrows, J. P., Degenstein, D., Froidevaux, L., and Thompson, A. M.: Stratospheric ozone trends and variability as seen by SCIAMACHY from 2002 to 2012, Atmos. Chem. Phys., 14, 831–846, doi:10.5194/acp-14-831-2014, 2014.

Hardiman, S. C., Butchart, N., Haynes, P. H., and Hare, S. H. E.: A note on forced versus internal variability of the stratosphere, Geophys. Res. Lett., 34, L12803, doi:10.1029/2007GL029726, 2007.

Jones, A., Urban, J., Murtagh, D. P., Eriksson, P., Brohede, S., Haley, C., Degenstein, D., Bourassa, A., von Savigny, C., Sonkaew, T., Rozanov, A., Bovensmann, H., and Burrows, J.: Evolution of stratospheric ozone and water vapour time series studied with satellite measurements, Atmos. Chem. Phys., 9, 6055–6075, doi:10.5194/acp-9-6055-2009, 2009.

Kawatani, Y. and Hamilton, K.: Weakened stratospheric quasibiennial oscillation driven by increased tropical mean upwelling, Nature, 497, 478–481, doi:10.1038/nature12140, 2013.

Konopka, P., Grooss, J.-U., Ploeger, F., and Mueller, R.: Annual cycle of horizontal in-mixing into the lower tropical stratosphere, J. Geophys. Res.-Atmos., 114, D19111, doi:10.1029/2009JD011955, 2009.

Kosaka, Y. and Xie, S.-P.: Recent global-warming hiatus tied to equatorial Pacific surface cooling, Nature, 501, 403–407, doi:10.1038/nature12534, 2013.

Kyrölä, E., Laine, M., Sofieva, V., Tamminen, J., Päivärinta, S.-M., Tukiainen, S., Zawodny, J., and Thomason, L.: Combined SAGE II–GOMOS ozone profile data set for 1984–2011 and trend analysis of the vertical distribution of ozone, Atmos. Chem. Phys., 13, 10645–10658, doi:10.5194/acp-13-10645-2013, 2013.

Li, F., Stolarski, R. S., Pawson, S., Newman, P. A., and Waugh, D.: Narrowing of the upwelling branch of the Brewer-Dobson circulation and Hadley cell in chemistry-climate model simulations of the 21st century, Geophys. Res. Lett., 37, L13702, doi:10.1029/2010GL043718, 2010.

Lin, M., Horowitz, L. W., Oltmans, S. J., Fiore, A. M., and Fan, S.: Tropospheric ozone trends at Mauna Loa Observatory tied to decadal climate variability, Nat. Geosci., 7, 136–143, doi:10.1038/ngeo2066, 2014.

Lin, P. and Fu, Q.: Changes in various branches of the Brewer–Dobson circulation from an ensemble of chemistry climate models, J. Geophys. Res.-Atmos., 118, 73–84, doi:10.1029/2012JD018813, 2013.

McCormick, M., Zawodny, J., Veiga, R., Larsen, J., and Wang, P.: An overview of SAGE-I and SAGE-II ozone measurements, Planet. Space Sci., 37, 1567–1586, doi:10.1016/0032-0633(89)90146-3, 1989.

Meehl, G. A., Arblaster, J. M., Fasullo, J. T., Hu, A., and Trenberth, K. E.: Model-based evidence of deep-ocean heat uptake during surface-temperature hiatus periods, Nat. Clim. Change, 1, 360–364, doi:10.1038/NCLIMATE1229, 2011.

Meul, S., Langematz, U., Oberländer, S., Garny, H., and Jöckel, P.: Chemical contribution to future tropical ozone change in the lower stratosphere, Atmos. Chem. Phys., 14, 2959–2971, doi:10.5194/acp-14-2959-2014, 2014.

Oman, L., Waugh, D. W., Pawson, S., Stolarski, R. S., and Newman, P. A.: On the influence of anthropogenic forcings on changes in the stratospheric mean age, J. Geophys. Res.-Atmos., 114, D03105, doi:10.1029/2008JD010378, 2009.

Ploeger, F., Fueglistaler, S., Grooß, J.-U., Günther, G., Konopka, P., Liu, Y.S., Müller, R., Ravegnani, F., Schiller, C., Ulanovski, A., and Riese, M.: Insight from ozone and water vapour on transport in the tropical tropopause layer (TTL), Atmos. Chem. Phys., 11, 407–419, doi:10.5194/acp-11-407-2011, 2011.

Ploeger, F., Konopka, P., Mueller, R., Fueglistaler, S., Schmidt, T., Manners, J. C., Grooss, J.-U., Guenther, G., Forster, P. M., and Riese, M.: Horizontal transport affecting trace gas seasonality in the Tropical Tropopause Layer (TTL), J. Geophys. Res.-Atmos., 117, D09303, doi:10.1029/2011JD017267, 2012.

Plumb, R.: A ‘’tropical pipe” model of stratospheric transport, J. Geophys. Res.-Atmos., 101, 3957–3972, doi:10.1029/95JD03002, 1996.

Polvani, L. M. and Solomon, S.: The signature of ozone depletion on tropical temperature trends, as revealed by their seasonal cycle in model integrations with single forcings, J. Geophys. Res.-Atmos., 117, D17102, doi:10.1029/2012JD017719, 2012.

Randel, W. J. and Jensen, E. J.: Physical processes in the tropical tropopause layer and their roles in a changing climate, Nat. Geosci., 6, 169–176, doi:10.1038/ngeo1733, 2013.

Randel, W. J. and Thompson, A. M.: Interannual variability and trends in tropical ozone derived from SAGE II satellite data and SHADOZ ozonesondes, J. Geophys. Res.-Atmos., 116, D07303, doi:10.1029/2010JD015195, 2011.

Randel, W. J., Wu, F., Voemel, H., Nedoluha, G. E., and Forster, P.: Decreases in stratospheric water vapor after 2001: links to changes in the tropical tropopause and the Brewer–Dobson circulation, J. Geophys. Res.-Atmos., 111, D12312, doi:10.1029/2005JD006744, 2006.

Reinsel, G. C., Weatherhead, E. C., Tiao, G. C., Miller, A. J., Nagatani, R. M., Wuebbles, D. J., and Flynn, L. E.: On detection of turnaround and recovery in trend for ozone, J. Geophys. Res.-Atmos., 107, 4078, doi:10.1029/2001JD000500, 2002.

Sander, S. P., Abbatt, J., Barker, J. R., Burkholder, J. B., Friedl, R. R., Golden, D. M., Huie, R. E., Kolb, C. E., Kurylo, M. J., Moortgat, G. K., Orkin, V. L., and Wine, P. H.: Chemical Kinetics and Photochemical Data for Use in Atmospheric Studies: Evaluation No. 17, JPL Publ. 10-6, Jet Propul. Lab., Pasadena, CA, 2011.

Seidel, D. J., Fu, Q., Randel, W. J., and Reichler, T. J.: Widening of the tropical belt in a changing climate, Nat. Geosci., 1, 21–24, doi:10.1038/ngeo.2007.38, 2008.

Seviour, W. J. M., Butchart, N., and Hardiman, S. C.: The Brewer–Dobson circulation inferred from ERA-Interim, Q. J. Roy. Meteor. Soc., 138, 878–888, doi:10.1002/qj.966, 2012.

Sinnhuber, B.-M., Weber, M., Amankwah, A., and Burrows, J. P.: Total ozone during the unusual Antarctic winter of 2002, Geophys. Res. Lett., 30, 1580, doi:10.1029/2002GL016798, 2003.

Sioris, C. E., McLinden, C. A., Fioletov, V. E., Adams, C., Zawodny, J. M., Bourassa, A. E., Roth, C. Z., and Degenstein, D. A.: Trend and variability in ozone in the tropical lower stratosphere over 2.5 solar cycles observed by SAGE II and OSIRIS, Atmos. Chem. Phys., 14, 3479–3496, doi:10.5194/acp-14-3479-2014, 2014.

Snow, M., Weber, M., Machol, J., Viereck, R., and Richard, E.: Comparison of Magnesium II core-to-wing ratio observations during solar minimum 23/24, J. Space Weather Space Clim., 4, A04, doi:10.1051/swsc/2014001, 2014.

Solomon, S., Kiehl, J. T., Garcia, R. R., and Grose, W.: Tracer transport by the diabatic circulation deduced from satellite-observations, J. Atmos. Sci., 43, 1603–1617, doi:10.1175/1520-0469(1986)043<1603:TTBTDC>2.0.CO;2, 1986.

Sonkaew, T., Rozanov, V. V., von Savigny, C., Rozanov, A., Bovensmann, H., and Burrows, J. P.: Cloud sensitivity studies for stratospheric and lower mesospheric ozone profile retrievals from measurements of limb-scattered solar radiation, Atmos. Meas. Tech., 2, 653–678, doi:10.5194/amt-2-653-2009, 2009.

Stiller, G. P., von Clarmann, T., Haenel, F., Funke, B., Glatthor, N., Grabowski, U., Kellmann, S., Kiefer, M., Linden, A., Lossow, S., and López-Puertas, M.: Observed temporal evolution of global mean age of stratospheric air for the 2002 to 2010 period, Atmos. Chem. Phys., 12, 3311–3331, doi:10.5194/acp-12-3311-2012, 2012.

Thompson, A. M., Witte, J. C., McPeters, R. D., Oltmans, S. J., Schmidlin, F. J., Logan, J. A., Fujiwara, M., Kirchhoff, V. W. J. H., Posny, F., Coetzee, G. J. R., Hoegger, B., Kawakami, S., Ogawa, T., Johnson, B. J., Vömel, H., and Labow, G.: Southern Hemisphere Additional Ozonesondes (SHADOZ) 1998–2000 tropical ozone climatology – 1. Comparison with Total Ozone Mapping Spectrometer (TOMS) and ground-based measurements, J. Geophys. Res.-Atmos., 108, 8238, doi:10.1029/2001JD000967, 2003.

Thompson, A. M., Miller, S. K., Tilmes, S., Kollonige, D. W., Witte, J. C., Oltmans, S. J., Johnson, B. J., Fujiwara, M., Schmidlin, F. J., Coetzee, G. J. R., Komala, N., Maata, M., Mohamad, M. B., Nguyo, J., Mutai, C., Ogino, S.-Y., Da Silva, F. R., Paes Leme, N. M., Posny, F., Scheele, R., Selkirk, H. B., Shiotani, M., Stuebi, R., Levrat, G., Calpini, B., Thouret, V., Tsuruta, H., Valverde Canossa, J., Voemel, H., Yonemura, S., Andres Diaz, J., Thanh, N. T. T., and Ha, H. T. T.: Southern Hemisphere Additional Ozonesondes (SHADOZ) ozone climatology (2005–2009): tropospheric and Tropical Tropopause Layer (TTL) profiles with comparisons to OMI-based ozone products, J. Geophys. Res.-Atmos., 117, D23301, doi:10.1029/2011JD016911, 2012.

Thompson, D. and Solomon, S.: Recent stratospheric climate trends as evidenced in radiosonde data: global structure and tropospheric linkages, J. Climate, 18, 4785–4795, doi:10.1175/JCLI3585.1, 2005.

Wang, H., Cunnold, D., Thomason, L., Zawodny, J., and Bodeker, G.: Assessment of SAGE version 6.1 ozone data quality, J. Geophys. Res.-Atmos., 107, 4691, doi:10.1029/2002JD002418, 2002.

Waugh, D. W., Oman, L., Kawa, S. R., Stolarski, R. S., Pawson, S., Douglass, A. R., Newman, P. A., and Nielsen, J. E.: Impacts of climate change on stratospheric ozone recovery, Geophys. Res. Lett., 36, L03805, doi:10.1029/2008GL036223, 2009.

Wolter, K. and Timlin, M. S.: El Nino/Southern Oscillation behaviour since 1871 as diagnosed in an extended multivariate ENSO index (MEI.ext), Int. J. Climatol., 31, 1074–1087, doi:10.1002/joc.2336, 2011.

World Meteorological Organization: Scientific Assessment of Ozone Depletion: 2010, Global Ozone Research and Monitoring Project-Report No. 52, Geneva, Switzerland, 2011.

Young, P. J., Rosenlof, K. H., Solomon, S., Sherwood, S. C., Fu, Q., and Lamarque, J.-F.: Changes in stratospheric temperatures and their implications for changes in the Brewer–Dobson circulation, 1979–2005, J. Climate, 25, 1759–1772, doi:10.1175/2011JCLI4048.1, 2012.